

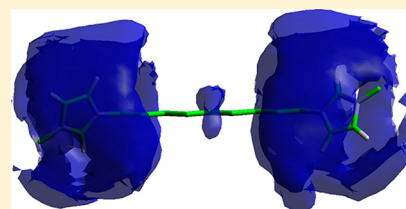
Molecular Dynamic Simulation of Dicationic Ionic Liquids: Effects of Anions and Alkyl Chain Length on Liquid Structure and Diffusion

Saeid Yeganegi,* Azim Soltanabadi, and Davood Farmanzadeh

Department of Physical Chemistry, Faculty of Chemistry, University of Mazandaran, Babolsar, Iran

S Supporting Information

ABSTRACT: Structures and dynamics of nine geminal dicationic ionic liquids (DILs) $C_n(\text{mim})_2X_2$, where $n = 3, 6$, and 9 and $X = \text{PF}_6^-$, BF_4^- , and Br^- , were studied by molecular dynamic simulations (*J. Phys. Chem. B* **2004**, *108*, 2038–2047). A force field with a minor modification for $C_3(\text{mim})_2 \times 2$ was adopted for the simulations. Densities, detailed microscopic structures, mean-square displacements (MSD), and self-diffusivities for various ion pairs from MD simulations have been presented. The calculated densities for $C_9(\text{mim})_2X_2$ ($X = \text{Br}^-$ and BF_4^-) agreed well with the experimental values. The calculated RDFs show that anions are well organized around the imidazolium rings. The calculated RDFs indicate that, unlike the mono cationic ILs, the anions and cations in DILs distribute homogeneously. Enthalpies of vaporization were calculated and correlated with the structural features of DILs. The local structure of $C_9(\text{mim})_2X_2$ ($X = \text{Br}$, PF_6) was examined by the spatial distribution function (SDF). The calculated SDFs show that similar trends were found by other groups for mono cationic ionic liquids (ILs). The highest probability densities are located around the imidazolium ring hydrogens. The calculated diffusion coefficients show that the ion diffusivities are 1 order of magnitude smaller than that of the mono cationic ionic liquids. The effects of alkyl chain length and anion type on the diffusion coefficient were also studied. The dynamics of the imidazolium rings and the alkyl chain in different time scales have also discussed. The calculated transference numbers show that the anions have the major role in carrying the electric current in a DIL.



1. INTRODUCTION

Room temperature ionic liquids (ILs) are a class of organic salts with melting points near room temperature.¹ In recent decades, there has been a tremendous growth in the interest in ionic liquids due to their individual and unique properties. The use and applications of ionic liquids have traversed many areas of chemistry and biochemistry.^{2–18} Due to their nonvolatility, thermal stability, and recyclability, ionic liquids are classified as green solvents.^{19–22} Compared with traditional organic solvents, ILs are environmentally benign and designable.²³ There are many combinations of different cations and anions, so one can design a specific ionic liquid for a specific application, which delivers an attractive feature to both academic institutes and industrial societies.^{24–35}

Geminal dicationic ionic liquids (DILs)³⁶ are a new family of ILs and consist of a doubly charged cation that is composed of two singly charged cations linked by an alkyl chain (also called a spacer) and paired with two singly charged anions. It is found that the geminal dicationic ILs possess a wider liquid range and higher thermal stability compared to traditional mono cationic ILs.^{37–40} Some applications of dicationic ILs have also been explored, such as stationary phases for gas chromatography,^{41–44} solvents for high-temperature organic reactions,⁴⁵ high-temperature lubricants,^{46–48} electrolytes in secondary batteries,^{49,50} and dye sensitized solar cells.^{51–53} Therefore, an estimation of the structure and electronic properties of the ions in DILs is important for designing new DILs for the specific applications. The development of a systematic method to select an ion pair for the rational design of new DILs is

essential for their application. For example, an estimation of the transport properties of the ions in the DILs is important for designing new DILs for electrolytes.⁵²

DILs have received very little attention from researchers compared to the monocationic ILs. There are few experimental studies on the dynamic properties of these compounds.^{54–57} The quantum mechanical studies on DILs are limited to one DFT computational calculation in the gas phase⁵⁸ and a semiempirical molecular modeling of interactions between DILs and a hydroxylated silicon surface.⁵⁹ Molecular dynamics simulation is a powerful tool for estimating the structure and transport properties of ionic liquids. However, the quality of the results of every simulation depends on the force field that should reproduce system properties accurately enough over a wide range of thermodynamic state. Very recently Dommert et al.⁶⁰ reviewed the classical force fields for the simulation of ionic liquids. They argued that the structural properties are modeled well by nonpolarizable force fields like Canongia-Lopes et al.⁶¹ and Liu et al.,⁶² but dynamic properties are strongly underestimated. A polarizable force field is essential to reproduce the dynamic properties. Either the polarization is exclusively modeled by a polarizable force field or a nonpolarizable force field by implicit treatment of polarization in terms of a reduced net charge, which requires much experimental information to parametrize the force field. Both

Received: June 18, 2012

Revised: August 15, 2012

Published: August 16, 2012



approaches are not practical for DILs now. Using polarizable force fields for simulations of DILs require huge computational resource due to the necessity of a smaller time-step, self-consistent calculation of the dipole moments and larger number of particles in a simulation box with respect to a mono cationic IL. The polarization effect can be included in force field in terms of the reduction of the net charge just as a further force-field parameter⁶⁰ and simply scaled down the electrostatic interactions globally to match the experimentally derived properties of the ionic liquids. However, for DILs there are not sufficient experimental data to be used in reliable adjusting the net and partial charges of the force field. Although the polarization effect in DILs can change the partial charges of the atoms, Bodo et al.⁶³ have shown that there is a qualitative similar trend between the ab initio calculated partial charges in DILs and those of the Canongia-Lopes⁶¹ force field.

As we are aware, there are few simulation studies on DILs.^{64–66} Bhargava et al.⁶⁴ studied the formation and structure of micellar aggregates in an aqueous solution of dicationic ionic liquid 1,3-bis(3-decylimidazolium-1-yl) propane bromide. In the second paper, Bhargava et al.⁶⁵ studied the structure and organization of the ions in the aqueous solutions of the same ionic liquid as their first paper by the coarse-grained molecular dynamics simulations. Recently, Bodo et al.⁶⁶ investigated the effect of linkage length on the local structure in the liquid phase of four ionic liquids composed by the geminal dications 1,3-bis[3-methylimidazolium-1-yl]alkane (alkane = propane, hexane, and nonane) and bis[(trifluoromethyl)sulfonyl] imide (Tf₂N) anion using the Canongia-Lopes et al.⁶¹ force field without any modification using MD simulations. They found that the two imidazolium rings of the same molecule do not interact with each other and do not show any particular orientation preference. In this work we will report, for the first time, the results of the MD simulations of liquid structure and ion diffusivities for nine dicationic ionic liquids 1,3-bis[3-methylimidazolium-1-yl]alkane (alkane = propane, hexane, and nonane) ($C_n(\text{mim})_2X_2$) ($n = 3, 6, \text{ or } 9$) where $X = \text{PF}_6^-$, BF_4^- , and Br^- . We have adopted the imidazolium force field of Canongia-Lopes et al.⁶¹ without any modification for $C_6(\text{mim})_2^{+2}$ and $C_9(\text{mim})_2^{+2}$ compounds but with a small modification of the cation atomic charges for $C_3(\text{mim})_2^{+2}$ compounds to account for the short alkyl chain between two imidazolium rings. In this paper, we first present the effect of the anion type and the alkyl linkage length on the density and microscopic structure of liquid phase, and then the results of calculations of ion diffusivities of the DILs will be presented.

2. SIMULATION DETAILS

The force field used in this work for $C_n(\text{mim})_2^{+2}X_2$ DILs was adapted from the all-atom force field developed by Canongia-Lopes et al.⁶¹ with a minor modification of atomic partial charges of the alkyl chain for the $C_3(\text{mim})_2^{+2}$ cation. The two imidazolium rings in the $C_3(\text{mim})_2^{+2}$ cation are connected to each other through a short linkage which can be made by replacement of one of the hydrogens of the end methyl group of 1-ethyl-3-methylimidazolium [$C_2\text{mim}^+$] by a methylene group of a 1,3-dimethylimidazolium [$C_1\text{mim}^+$] moiety. We adopted a method proposed by Bhargava et al.⁶⁴ that the residual charge (due to the replacement of the third hydrogen atoms of 3-methyl groups by a methylene group) has been distributed to the hydrogen atoms (+0.125e each, where e is the electron charge) of the central methylene group of the spacer to preserve the net charge +2 of the cation and the symmetry of

atomic charge in the alkyl linkage. For $C_6(\text{mim})_2^{+2}$ and $C_9(\text{mim})_2^{+2}$ the Canongia-Lopes et al.⁶¹ force field has been utilized without any modification. The atomic partial charges used in this work are presented in Table 1. The values of the other force field parameters are taken from Canongia-Lopes et al.⁶¹ without any changes.

Table 1. Partial Charge on Each Atom of $C_3(\text{mim})_2^{+2}$, $C_6(\text{mim})_2^{+2}$, and $C_9(\text{mim})_2^{+2}$ Cations^a

atom type	q_i/e^b		
	$C_3(\text{mim})_2^{+2}$	$C_6(\text{mim})_2^{+2}$	$C_9(\text{mim})_2^{+2}$
NA1	0.15	0.15	0.15
CR2	−0.11	−0.11	−0.11
NA3	0.15	0.15	0.15
CW4	−0.13	−0.13	−0.13
CW5	−0.13	−0.13	−0.13
C0	−0.17	−0.17	−0.17
C1	−0.17	−0.17	−0.17
C2	0.01	0.01	0.01
C3		−0.12	−0.12
C4		−0.12	−0.12
CT		−0.12	−0.12
H0	0.13	0.13	0.13
H1	0.13	0.13	0.13
H2	0.01 ^c	0.06	0.06
H3		0.06	0.06
H4		0.06	0.06
HT		0.06	0.06
H8	0.21	0.21	0.21
H9	0.21	0.21	0.21
H10	0.21	0.21	0.21

^aThe H0, H1, H2, H3, H4, and HT show the hydrogen connected to C0, C1, C2, C3, C4, and CT, respectively. ^bReference 61. ^cReference 65

The minimum-energy geometry of the anions and cations for the $C_n(\text{mim})_2X_2$ ($n = 3, 6, \text{ and } 9$ and $X = \text{Br}^-$, BF_4^- , and PF_6^-) was determined by performing density functional theory geometry optimization on the isolated cation and anion at the B3LYP/6-31++G** level of theory using Gaussian 03.⁶⁷ An additional vibration analysis was followed to ensure the absence of negative frequencies and verify the existence of a true minimum. The cation and anion charges were set at +2 and −1, respectively. The schematic structures of studied DILs are shown in Figure 1.

Molecular dynamic simulations have been carried out on nine DILs cations joined by alkyl linkage chains of different lengths with three different anions PF_6^- , BF_4^- , and Br^- using DL-poly 2.20 code.⁶⁸ The simulated fluids consist of 120–180 ionic complexes (120–180 cations and 240–360 anions). Initial configurations were generated by placing sufficient replicas of optimized ion triplet (one dication and two anions) in three dimensions in the simulation box. Simulations were performed with the Nosé–Hoover thermostat and barostat algorithm.^{69,70} The relaxation times used for the thermostat and barostat are 0.1 and 0.5 ps, respectively. Periodic boundary conditions were employed, and equations of motion were integrated using the Verlet leapfrog scheme.⁷¹ All intermolecular interactions between atoms in the simulation box were calculated within a cutoff distance of $R_{\text{cutoff}} = 14.0 \text{ \AA}$ for all simulated systems. The electrostatic long-range interactions were calculated using the Ewald summation method⁷¹ with a

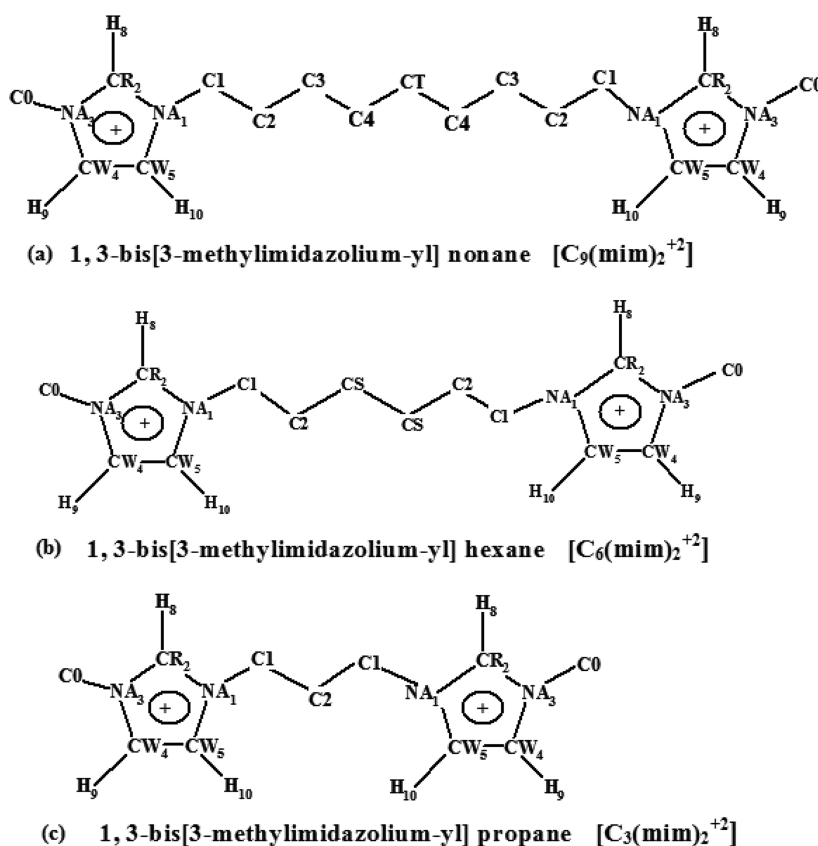


Figure 1. Schematic structure of dications in geminal dicationic ionic liquids simulated in this study. The H0, H1, H2, H3, H4, and HT do not show and represent hydrogen connected to C0, C1, C2, C3, C4, and CT, respectively.

precision of 1×10^{-6} . The time step for all of the simulations was set as 1.0 fs. All of the simulations were done at $P = 1.0$ atm and $T = 450$ K in order to ensure that all compounds are liquid. The simulations were started in NPT ensemble at a much higher temperature, 800 K and low density. The system was equilibrated for 500 ps, then the temperature was gradually lowered to 600 K, and finally lowered to 450 K where simulations were conducted for 500 ps at each temperature. Anderson et al.³⁶ have reported the experimental melting points of the $\text{C}_n(\text{mim})_2\text{X}_2$ ($\text{X} = \text{PF}_6^-$, BF_4^- , and Br^-) DIL series. The reported melting points are generally about 400 K. $\text{C}_3(\text{mim})_2\text{Br}_2$ has the highest melting point (435 K) among the other DILs.³⁶ Then, we have performed all simulations at 450 K to ensure that all DILs are liquid. For calculation of the equilibrium densities, the simulation has been continued for another 1 ns and results of the last step (450 K) were gathered for analysis. The mean square displacement MSDs were averaged over a set of three NVT simulations each with a total 0.5 ns equilibration followed by a 10 ns production in which the positions of particles were recorded every 0.2 ps. The starting point of each NVT simulation was an equilibrated final configuration of a relevant NPT simulation. By the end of the equilibration, the total energies and volumes were monitored until the corresponding time series were stationary.

3. RESULTS AND DISCUSSION

3.1. Liquid Structure. Densities of ionic liquids are one of the most accurate sources of experimental data. Anderson et al.³⁶ measured the densities of $\text{C}_9(\text{mim})_2(\text{BF}_4)_2$ and $\text{C}_9(\text{mim})_2(\text{Br})_2$ at 296 K and 1 atm as 1.33 and 1.41 g/cm^3 , respectively. The computed densities of $\text{C}_9(\text{mim})_2(\text{BF}_4)_2$ and

$\text{C}_9(\text{mim})_2(\text{Br})_2$ using NPT simulations at 296 K and 1 atm were 1.35 and 1.43 g/cm^3 , respectively. The predicted densities for $\text{C}_9(\text{mim})_2(\text{BF}_4)_2$ and $\text{C}_9(\text{mim})_2(\text{Br})_2$ are larger than the experimental densities³⁶ by less than 1.5%. This level of agreement is excellent considering that the calculations are purely predictive; none of the force field parameters have been adjusted to match experimental data.

Densities of all nine DILs were calculated by NPT simulations at 450 K and 1 atm and results are shown in Table 2. Also, Figure 2 represents the calculated densities of

Table 2. Computed Liquid Densities of Nine Studied DILs at 450 K and 1 atm

DILs	ρ (g/cm^3)
$\text{C}_3(\text{mim})_2(\text{Br})_2$	1.48 ₈
$\text{C}_3(\text{mim})_2(\text{BF}_4)_2$	1.27 ₉
$\text{C}_3(\text{mim})_2(\text{PF}_6)_2$	1.47 ₉
$\text{C}_6(\text{mim})_2(\text{Br})_2$	1.37 ₃
$\text{C}_6(\text{mim})_2(\text{BF}_4)_2$	1.20 ₇
$\text{C}_6(\text{mim})_2(\text{PF}_6)_2$	1.38 ₁
$\text{C}_9(\text{mim})_2(\text{Br})_2$	1.27 ₅
$\text{C}_9(\text{mim})_2(\text{BF}_4)_2$	1.15 ₁
$\text{C}_9(\text{mim})_2(\text{PF}_6)_2$	1.31 ₃

DILs studied in this work versus the alkyl chain length. According to Figure 2, densities decrease with the number of carbon atoms. As shown in Figure 2, the densities of the DILs were found to be cation and anion dependent and decrease with the length of the alkyl linkage chain. Decreasing of the density with increasing alkyl chain length has been reported

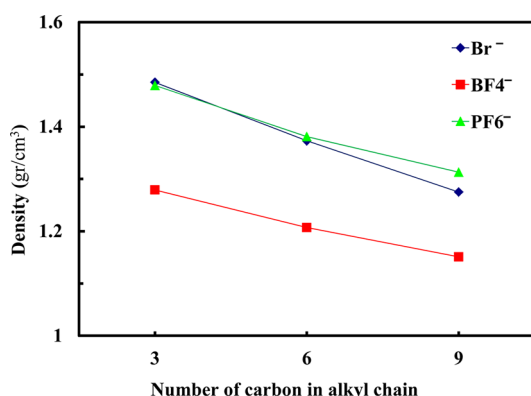


Figure 2. Calculated densities of $[(C_n(\text{mim})_2X_2)]$, $n = 3, 6$, and 9 and $X = \text{PF}_6^-$, BF_4^- , and Br^- ionic liquids at 450 K and 1 atm . Lines are drawn to guide the eyes.

previously^{72,73} for a large series of 1-alkyl-3-methylimidazolium ionic liquids. The order of densities of DILs, in Table 2, for a particular cation approximately follows the decreasing order of the molecular weight of the anions $\text{PF}_6^- > \text{Br}^- > \text{BF}_4^-$, a similar trend has been observed in mono cationic ILs.⁷⁴

The vaporization of the mono cationic ILs has been successfully studied and the vapor was shown to consist of neutral ion pairs.^{75–77} Lovelock et al.⁷⁸ studied the vapor phase of the dicationic ionic liquid 1,3-bis(3-methylimidazolium-1-yl) propane bis(trifluoromethanesulfonyl)-imide, $[\text{C}_3(\text{mim})_2][\text{NTf}_2]_2$, by temperature-programmed desorption (TPD), coupled with line-of-sight mass spectrometry (LOS-MS). They showed that vapor phase of an aprotic dicationic ionic liquid is composed of neutral ion triplets (one cation attached to two anion). Their result was later confirmed by Vitorino et al.⁷⁹ by a different experimental method (an ion-cyclotron resonance mass spectroscopy technique) and also the molecular dynamics simulations.

Enthalpy of vaporization ΔH_{vap} , also known as the heat of vaporization or heat of evaporation, is the energy required to transform a given quantity of a liquid into gas at a given pressure. It is difficult to measure the enthalpy of vaporization of DILs directly from experiment, since all DILs are nonvolatile. The enthalpy of vaporization, ΔH_{vap} , calculated as follows:

$$\Delta H_{\text{vap}} = RT - (U_{\text{int}} - U_{\text{ion triplet}}) \quad (1)$$

where R is the gas constant, T is the absolute temperature, U_{int} is the average of energy per mole of an ion triplet in the liquid, and $U_{\text{ion triplet}}$ represents the average internal energy of an neutral ion triplet in the gas state. The $U_{\text{ion triplet}}$ was calculated by simulations of a dication and two anions in a large simulation box⁸⁰ and averaging the energy over the simulated ion triplets.

Unfortunately, the lack of experimental data for heat of vaporizations does not allow a quantitative comparison. However, the simulation studies allow investigation of the influence of van der Waals and Coulombic interactions on the heats of vaporization. Table 3 shows the calculated ΔH_{vap} for nine studied DILs as well as van der Waals and Coulombic contributions to the interaction of an ionic triplet in the liquid. Due to the strong interactions in DILs, the calculated ΔH_{vap} is generally larger than that of the mono cationic ionic liquids.^{8,81} The calculated ΔH_{vap} decreases with the carbon number of linkage, which is a result of the weaker electrostatic interactions between cations and anions. The larger alkyl chain increases the

Table 3. Simulated Heats of Vaporization of DILs and the van der Waals and Coulombic Contributions to the Heats of Vaporization in the Liquid State at 450 K and 1 atm ^a

	ΔH_{vap}	$\Delta U_{\text{Coulomb}}$	ΔU_{vdw}
$\text{C}_3(\text{mim})_2\text{Br}_2$	295 ± 2.8	-196 ± 1	-96.1 ± 1
$\text{C}_6(\text{mim})_2\text{Br}_2$	263 ± 3.0	-180 ± 1	-106 ± 1
$\text{C}_9(\text{mim})_2\text{Br}_2$	253 ± 3.5	-147 ± 1	-117 ± 1
$\text{C}_3(\text{mim})_2(\text{BF}_4)_2$	246 ± 2.5	-180 ± 1	-98 ± 1
$\text{C}_6(\text{mim})_2(\text{BF}_4)_2$	222 ± 3.2	-141 ± 1	-98 ± 1
$\text{C}_9(\text{mim})_2(\text{BF}_4)_2$	200 ± 3.2	-147 ± 1	-110 ± 1
$\text{C}_3(\text{mim})_2(\text{PF}_6)_2$	1280 ± 3.4	-180 ± 1	-218 ± 1
$\text{C}_6(\text{mim})_2(\text{PF}_6)_2$	558 ± 2.5	-116 ± 1	-98 ± 1
$\text{C}_9(\text{mim})_2(\text{PF}_6)_2$	145 ± 3.8	-129 ± 1	-111 ± 1

^aAll energies are given in kJ mol^{-1} .

van der Waals interaction, but at the same time, it can decrease the electrostatic interaction by screening effect. Bodo et al.⁶⁶ have shown that for DILs in liquid phase the alkyl chain is elongated so increasing the alkyl chain length causes larger separation between the anions around a ring and the other ring in the same molecule, which in turn reduce the electrostatic interaction.

We investigated the liquid structure by calculating various radial distribution functions (RDFs or $g(r)$) of ions over the 10.0 ns of the trajectories at 450 K and 1 atm as well as the spatial distribution function (SDF) of anions around the cations. The calculated RDFs for anion-geometric center of imidazolium rings of cation, anion-anion and cation-cation center-of-mass are shown in Figure 3. The simulated RDFs for the anions around geometric center of imidazolium rings in Figure 3a–c shows that there is a first sharp peak at about $4.6\text{--}5.3\text{ \AA}$ and a second broad peak at about $10\text{--}10.7\text{ \AA}$ which imply that the anion is very well organized around the cation rings. The systematic distance of $5\text{--}6\text{ \AA}$ between the positions of the first and second peaks can be associated with the solvation shells for both cation and anion. All of the correlation exhibits long-range spatial correlations that extend beyond 1.4 nm , a feature that has been observed in simulations of other ionic liquid systems. These observed ordering agree remarkably with previous works for mono cationic ILs.^{82,83} Furthermore, from Figure 3a–c, one can see that the distribution of anions around the imidazolium rings is the same for a particular anion and it is insensitive to the cation type. This finding is due to the fact that the preferred location of finding anions is above or below the ring plane. However, by changing the anion type from Br^- to BF_4^- and PF_6^- for a specific cation, the first and second peaks shift to longer distances due to the size effect of anions as the order of $\text{PF}_6^- > \text{BF}_4^- > \text{Br}^-$.

The RDFs of cation-cation in Figure 3d–f show very broad peaks. The cation-cation RDFs for $\text{C}_3(\text{mim})_2$ show a broad first peak at about 7 \AA , but for larger cations the calculated RDFs lack a well-defined first peak. This is expected because the geminal ionic liquids have bulky cations. Anion-anion RDFs are presented in Figure 3g–i and they show a first peak around 6 \AA with a second peak at distances larger than 12 \AA , again the distance of 6 \AA between the position of first and second peaks can be associated with solvation shells for both cation and anions. The anion-anion RDFs for different cations are similar and changing the cation type has no effect on the anion-anion RDFs.

To elaborate the more detailed structure of anions around the imidazolium ring, we have calculated the RDFs of anion

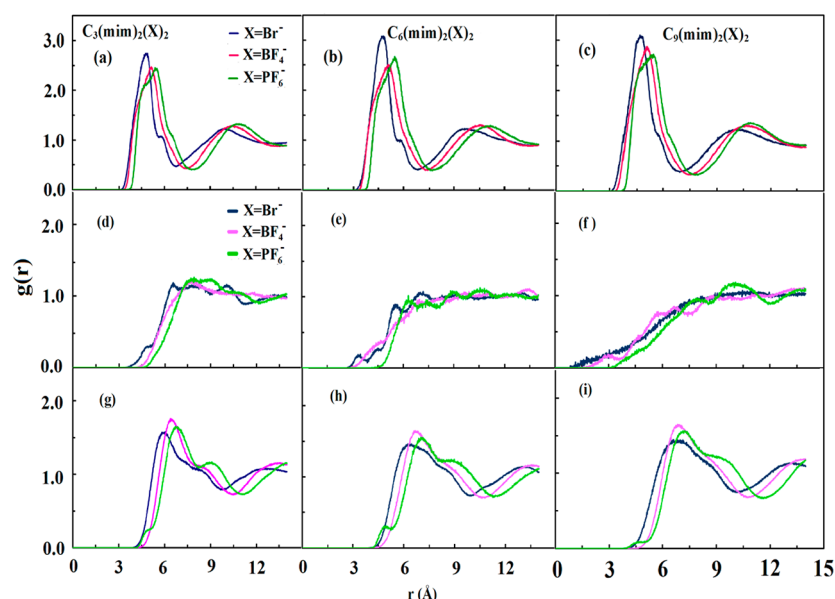


Figure 3. Calculated radial distribution functions for ring–anion (a–c), cation–cation (d–f), and anion–anion (g–i) correlations for $[\text{C}_n(\text{mim})_2\text{X}_2]$, $n = 3, 6$, and 9 and $\text{X} = \text{PF}_6^-$, BF_4^- , and Br^- ionic liquids at 450 K and 1 atm .

PF_6^- and hydrogen atoms (H8, H9, and H10 in Figure 1a) of the imidazolium rings for $\text{C}_9(\text{mim})_2(\text{PF}_6)_2$ and shown in Figure 4. The well-defined peaks at about 3.5 Å in Figure 4 indicate

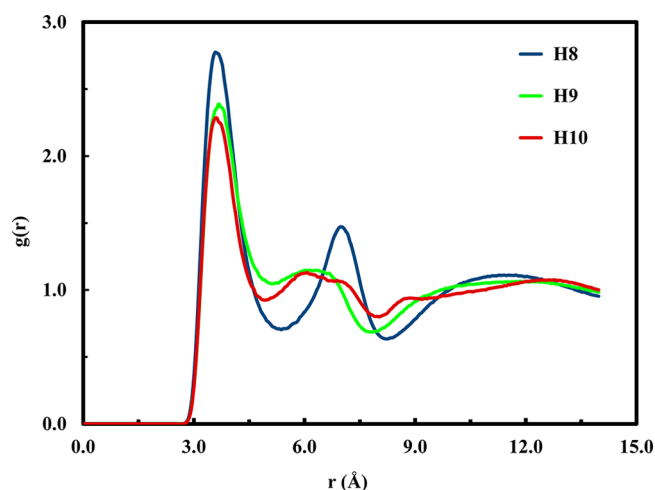


Figure 4. Radial distribution function of anion PF_6^- around the rings atom H8, H9, and H10 for $\text{C}_9(\text{mim})_2(\text{PF}_6)_2$ at 450 K and 1 atm . The labels are defined according to Figure 1.

the strong interactions between these hydrogens and fluorine atoms of the anions. Furthermore, the position and sharpness of these RDFs indicate that these correlations can be related to an interaction between these charged sites.^{64,84} However, the differences in the amplitude of the obtained RDFs indicate that the H8 hydrogen site has the strongest interaction among other ring hydrogen's. Similar results were observed and reported in imidazolium derived mono cationic ILs.⁸⁵ The nature of the interaction between hydrogens of the imidazolium ring and anion has been the subject of controversial discussions in recent years.^{86–91} Kanzaki et al.⁹¹ studied the ion–ion interaction in 1-ethyl-3-methylimidazolium tetrafluoroborate by large angle X-ray scattering experiment and MD simulations. They concluded that the characteristics of “weak interaction” of the hydrogens

of the ring and anions are considerably different from that of the conventional hydrogen bonds. However, very recently Dong and Zhang⁹⁰ reviewed the hydrogen bonding in ionic liquids and stated that hydrogen bonds exist in many different ILs and have a crucial effect on their properties.

The second peak for H8- PF_6^- RDF at 7 Å can be attributed to the correlation with second shell anions. However, the second peaks for H9- PF_6^- and H10- PF_6^- in Figure 4 are much broader and shifted to the smaller distances with respect to the second peak for H8- PF_6^- . This can be attributed to the fact that the first shell of anions around H9 (or H10) has some contribution from the second shell of anions for H9 (or H10). The RDF of anion PF_6^- around the alkyl chain for atoms C1, C2, C3, C4, and CT in $\text{C}_9(\text{mim})_2(\text{PF}_6)_2$ are shown in Figure 5. According to Figure 5, the peaks get shorter and broader as the anion moves from the imidazolium ring toward center of alkyl chain (CT).

The calculated radial distribution function of geometric centers of imidazolium rings of two distinct cations for all nine studied dicationic ionic liquids are shown in Figure 6. The pronounced feature in all of these RDFs is the observation of a very broad first peak at $6\text{--}7\text{ Å}$ and a second peak beyond the 14

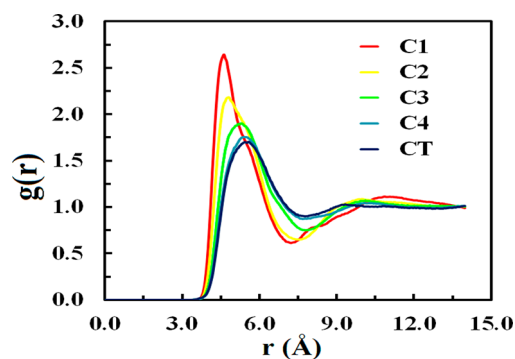


Figure 5. Radial distribution functions of anion PF_6^- around the alkyl chain atoms C1, C2, C3, C4, and CT (for labels refer to those in Figure 1a) for $\text{C}_9(\text{mim})_2(\text{PF}_6)_2$ at 450 K and 1 atm .

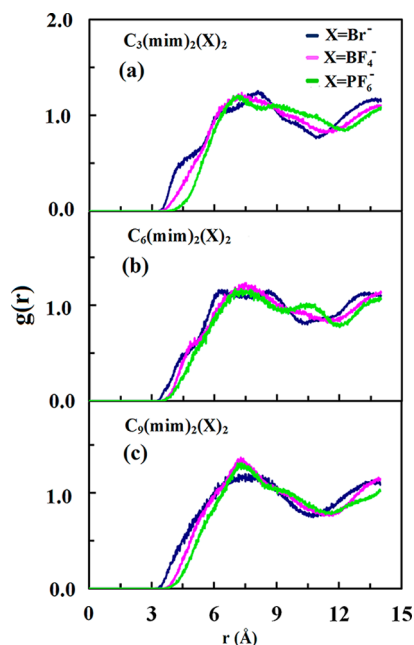


Figure 6. Radial distribution function of geometric center of imidazolium ring–ring correlation for different cations at 450 K and 1 atm for $C_3(\text{mim})_2X_2$ (a), $C_6(\text{mim})_2X_2$ (b), and $C_9(\text{mim})_2X_2$ (c). X denotes the anion.

Å (the cutoff distance). These correlations indicate that the anions and head groups of the cations distribute homogeneously because of the strong electrostatic interactions.

Though qualitative, more intuitive structures were obtained from the SDFs, which give the probability of finding an atom in three-dimensional space around a center molecule, in contrast to the average values given by RDF. SDFs visualized by the software package Aten⁸² are shown in Figures 7 and 8. The

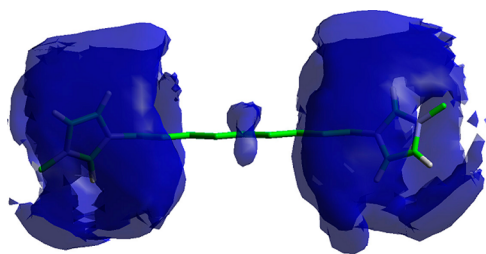


Figure 7. Spatial distribution functions of anions around the cation for $C_9(\text{mim})_2(\text{PF}_6)_2$ at 450 K. The surface is drawn at six times the average density.

spatial distribution of the anion (phosphorus) around cation for $C_9(\text{mim})_2(\text{PF}_6)_2$ is depicted in Figure 7. As expected, the probability of finding anions around the imidazolium rings is higher than that for around the alkyl chain, and the anions most likely cluster around the rings. However, there is also a small region of high density in the middle of the alkyl chain which is in line with the other simulation studies.^{72,93} To be more specific, the SDFs of the anion around an imidazolium ring for $C_9(\text{mim})_2X_2$ ($X = \text{Br}^-$ and PF_6^-) are shown in Figure 8. The calculated SDFs have the main features of the reported SDFs for mono ILs by other researchers.^{83,93–97} There exist three regions with a high probability of finding the anions: (1) around the CR2–H8 group, both above and below the plane of the imidazolium ring; (2) between CW4–H9 and methyl groups;

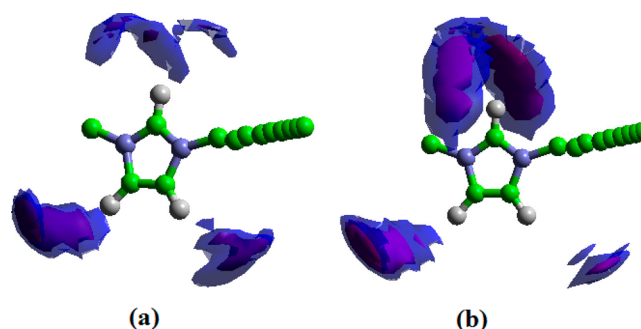


Figure 8. Spatial distribution functions of anions around the imidazolium ring for (a) $C_9(\text{mim})_2\text{Br}_2$ and (b) $C_9(\text{mim})_2(\text{PF}_6)_2$. The surface is drawn at 16 (purple) and 6 (blue) times the average density. The second imidazolium ring and the hydrogens of the alkyl chains were omitted for clarity.

and (3) between CW5–H10 and alkyl side chain. The SDF of $C_9(\text{mim})_2(\text{Br})_2$ in Figure 8a is very similar to the calculated one by Raabe et al.⁹³ for (hmim)(Cl). Also the SDF of the $C_9(\text{mim})_2(\text{PF}_6)_2$ in Figure 8b is completely similar to the calculated SDFs of [bmim][PF₆] by Bhargava et al.⁹⁶ and Liu et al.^{72,97} Although the SDFs in Figure 8 have similar characteristics, there are remarkable differences in the SDFs of Br^- and PF_6^- anions around the ring. A pronounced difference between the distribution of the Br^- and PF_6^- anions around the ring is that the very high density area (the red region which refer to 13 time average density) exists in all three regions for $C_9(\text{mim})_2\text{Br}_2$, but only around the CR2 for $C_9(\text{mim})_2(\text{PF}_6)_2$. The other important difference is that the SDF of the PF_6^- anions is divided below and above the ring as the anion changes from PF_6^- to Br^- , because of the anion size. This observation agrees well with the results from previous studies on the mono ILs.^{93,97,98} The different shapes of the high probability density of SDFs in Figure 8 can be explained in terms of the low charge density and the larger size of the PF_6^- anion. Our results show that the spatial distribution of anions around the imidazolium rings in DILs is not different from their mono cationic ILs counterparts.

3.2. Diffusion Coefficient. The self-diffusion coefficient of a fluid can be calculated using the Einstein equation.

The self-diffusion coefficient, D , can be calculated by the Einstein relation⁹⁹

$$D_{\text{self}} = \frac{1}{6} \lim_{t \rightarrow \infty} \frac{d}{dt} \left\langle [r_i(t) - r_i(0)]^2 \right\rangle \quad (2)$$

where the quantity in braces is the ensemble-averaged mean square displacement (MSD) of the molecules and r_i is the vector coordinate of the center of mass of ion i . The trajectories were dumped for 10 ns every 200 fs at 450.0 K after 1 ns equilibration and the self-diffusion coefficients obtained from the slopes of the line fitted to the MSDs in the range 3–8.5 ns.

The mean squared displacements (MSD) regarding NVE simulations of nine dicationic ionic liquids for center of mass of cations and anions up to a time of 8.5 ns are shown in Figure 7 for all nine studied DILs. The influence of alkyl chain length on anion MSDs and the effect of the anion size on cation MSDs are shown in Figure 7, panels a–c and d–f, respectively. The log–log plots of the MSDs of the ions in the nine ionic liquids are shown in Figures S1–S9 in the Supporting Information. The initial rapid increase of calculated MSDs in Figure 7 continues until 3 ns, which shows that a sufficiently long

simulation is necessary for an accurate evaluation of the self-diffusion coefficients of the ions in the ionic liquid. The asymptotic linear regions ($t > 3$ ns) were used for the calculation of the diffusion coefficients.

According to Figure 9, all MSD curves are linear after the initial 3 ns. The self-diffusion has been calculated in the time

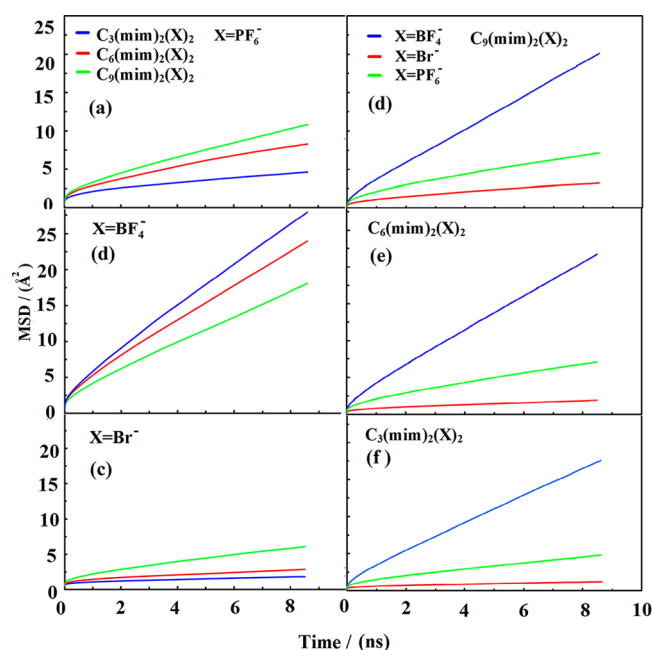


Figure 9. Calculated MSDs of anions (three different cations with the same anions (left)) and cations (one cation with the three anions (right)) at 450 K and 1 atm.

ranges of 3–6, 4–7, 5–8, and 3–8 ns, where the results are presented in Table 4. It can be seen from Table 4 that there is no significant difference between the calculated diffusion coefficients for different time ranges. The calculated values of diffusion coefficients in Table 4 are typically 1 order of magnitude smaller than that of mono cationic ILs with a comparable molar mass. For example, the calculated diffusion coefficients of cation and anion for $C_3(\text{mim})_2(\text{BF}_4)_2$ (cation mass = 206 au) is $0.3 \times 10^{-11} \text{ m}^2/\text{s}$ (Table 4) which can be compared with that of $[\text{C}_8\text{mim}][\text{BF}_4]$ (cation mass = 195 au) calculated by Tsuzuki et al.¹⁰⁰ at 353 K as 9.0×10^{-11} and $8.8 \times 10^{-11} \text{ m}^2/\text{s}$ for the cation and anion, respectively. Our results show that a DIL has a much smaller self-diffusion coefficients than a mono cationic IL with a mass comparable cation. This can be understood if one notes that the densities of DILs and mono cationic ILs are not so much different, for example the experimental densities¹⁰¹ of $[\text{C}_4\text{mim}][\text{BF}_4]$ and $[\text{C}_4\text{mim}][\text{PF}_6]$ are 1.096 and 1.247 g/cm³ at 452 K which is comparable with the calculated densities of studied DILs in Table 2. The charge density in a DIL is two times larger than that of a corresponding mono cationic IL with the same number of cations and comparable density. Tsuzuki et al.¹⁰² showed that the D_{cation} and D_{anion} obtained from the molecular dynamics simulations of mono cationic ILs without the electrostatic interactions are about 40 times larger than those obtained from the simulation with the electrostatic interactions. The strengthen of electrostatic interaction in the DILs can account for the large decrease of the D_{cation} and D_{anion} in the DILs relative to a mono cationic IL. On the basis of the results of

Table 4. Calculated Diffusion Coefficient of Cations and Anions from the Slope of MSD Plots in Figure 8 for 3–6, 4–7, 5–8, and 3–8 ns Time Ranges and Calculated Transfers Number for Nine Dicationic Ionic Liquids at 450 K and 1.0 atm

DILs molecule	D^- ($10^{-11} \text{ m}^2/\text{s}$)				t_*
	3–6 ns	4–7 ns	5–8 ns	3–8 ns	
$C_3(\text{mim})_2(\text{BF}_4)_2$	0.283	0.300	0.300	0.300	0.655
$C_6(\text{mim})_2(\text{BF}_4)_2$	0.400	0.400	0.400	0.400	0.676
$C_9(\text{mim})_2(\text{BF}_4)_2$	0.483	0.483	0.483	0.483	0.725
$C_3(\text{mim})_2(\text{Br})_2$	0.017	0.015	0.013	0.016	0.727
$C_6(\text{mim})_2(\text{Br})_2$	0.033	0.033	0.033	0.033	0.800
$C_9(\text{mim})_2(\text{Br})_2$	0.083	0.083	0.073	0.080	0.772
$C_3(\text{mim})_2(\text{PF}_6)_2$	0.050	0.050	0.050	0.050	0.600
$C_6(\text{mim})_2(\text{PF}_6)_2$	0.133	0.107	0.107	0.117	0.681
$C_9(\text{mim})_2(\text{PF}_6)_2$	0.167	0.150	0.150	0.150	0.750
DILs molecule	D^+ ($10^{-11} \text{ m}^2/\text{s}$)				t_*
	3–6 ns	4–7 ns	5–8 ns	3–8 ns	
$C_3(\text{mim})_2(\text{BF}_4)_2$	0.300	0.302	0.317	0.300	0.345
$C_6(\text{mim})_2(\text{BF}_4)_2$	0.383	0.383	0.383	0.383	0.324
$C_9(\text{mim})_2(\text{BF}_4)_2$	0.367	0.367	0.367	0.367	0.275
$C_3(\text{mim})_2(\text{Br})_2$	0.013	0.012	0.010	0.012	0.273
$C_6(\text{mim})_2(\text{Br})_2$	0.017	0.017	0.017	0.017	0.200
$C_9(\text{mim})_2(\text{Br})_2$	0.050	0.050	0.043	0.050	0.228
$C_3(\text{mim})_2(\text{PF}_6)_2$	0.067	0.067	0.067	0.067	0.400
$C_6(\text{mim})_2(\text{PF}_6)_2$	0.117	0.100	0.100	0.100	0.319
$C_9(\text{mim})_2(\text{PF}_6)_2$	0.117	0.100	0.100	0.100	0.250

simulation of the mono cationic ILs by other researchers,^{103,104} it is well accepted that a nonpolarizable force field underestimates the self-diffusion coefficient. Therefore, we suggest that the inclusion of polarization in the force field will improve the simulation results, but the trends of the calculated diffusion coefficients remain unchanged.

The influence of the alkyl chain length on the calculated diffusion coefficients in Table 5 show that, contrary to the

Table 5. Calculated Diffusion Coefficient for the Cations, CT (Central Atom Between Two Imidazolium Rings in Figure 1), and Imidazolium Rings from the Slope of Calculated MSDs in Figure 7 for Nine DILs at 450 K and 1.0 atm

DILs molecule	D^+ ($10^{-11} \text{ m}^2/\text{s}$)	D^{CT} ($10^{-11} \text{ m}^2/\text{s}$)	D^{ring} ($10^{-11} \text{ m}^2/\text{s}$)
	cation	CT	ring
$C_3(\text{mim})_2(\text{BF}_4)_2$	0.300	0.333	0.500
$C_6(\text{mim})_2(\text{BF}_4)_2$	0.383	0.433	0.683
$C_9(\text{mim})_2(\text{BF}_4)_2$	0.367	0.483	0.700
$C_3(\text{mim})_2(\text{Br})_2$	0.012	0.033	0.033
$C_6(\text{mim})_2(\text{Br})_2$	0.017	0.033	0.050
$C_9(\text{mim})_2(\text{Br})_2$	0.050	0.083	0.083
$C_3(\text{mim})_2(\text{PF}_6)_2$	0.067	0.100	0.117
$C_6(\text{mim})_2(\text{PF}_6)_2$	0.100	0.150	0.200
$C_9(\text{mim})_2(\text{PF}_6)_2$	0.100	0.167	0.233

observed trend in mono cationic ILs, the D_{cation} increases with the alkyl chain length. The lengthening of the alkyl chain causes a dispersion of the charge centers and weakening the electrostatic attractions between cations and anions, but at the same time, it enhances the total strength of the van der Waals interactions. The balance between these opposing effects

of side chain lengthening determines the dynamics of ions. From Table 2, one can see that the density of DILs decreases with alkyl chain length. This suggests that the low density is also responsible for increasing the calculated self-diffusion coefficients of ions with longer alkyl chain.

The observed trend for the diffusion coefficients of anions in Table 4 is $\text{BF}_4^- > \text{PF}_6^- > \text{Br}^-$ which is in agreement with the observed trend in mono cationic ILs.^{100,105} The observed trend for the anions diffusion coefficients can be explained in terms of the size and mass of the anions. The PF_6^- anion is the largest of the three anions and has the lowest surface charge density, whereas Br^- has the highest surface charge density due to its small size. Also one note that in Figure 2 the $\text{C}_n(\text{mim})_2(\text{BF}_4)_2$ DILs has lower density than the $\text{C}_n(\text{mim})_2\text{Br}_2$ and $\text{C}_n(\text{mim})_2(\text{PF}_6)_2$ DILs. For the BF_4^- anion, there is a compromise between size and mass. Its mass is nearly equal to Br^- , but its size is larger than that of Br^- , which results in a lower density and larger diffusion coefficient.

In the next step, we explored the dynamics of the ring and the alkyl chain atoms in the DILs. Tsuzuki and co-workers¹⁰⁰ showed that the translational dynamics of the alkyl chain and the imidazolium ring in mono cationic ILs is approximately the same on a large time scale. On the other hand, the motion of the carbon atoms in the alkyl chain is faster than that of the atoms in the imidazolium rings in the smaller time scales. To shed light on the dynamics of the cation atoms, the calculated MSDs of the geometric center of imidazolium rings and the carbon atom in the middle of the alkyl chain (CT for $\text{C}_9(\text{mim})_2^{+2}$, CS for $\text{C}_6(\text{mim})_2^{+2}$, and C2 for $\text{C}_3(\text{mim})_2^{+2}$), for all DILs from 8.5 ns simulations at 450 K, are depicted in Figure 10. The numbering of atoms is shown in Figure 1. The

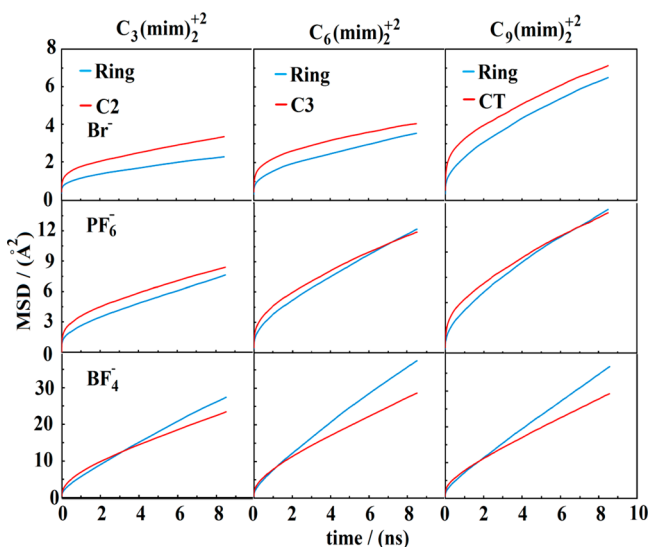


Figure 10. Calculated MSDs of the geometric center of imidazolium rings and the carbon atom in the middle of the alkyl chain (CT for $\text{C}_9(\text{mim})_2^{+2}$, CS for $\text{C}_6(\text{mim})_2^{+2}$, and C2 for $\text{C}_3(\text{mim})_2^{+2}$), for all DILs at 450 K and 1.0 atm.

calculated diffusion coefficients based on the MSDs in Figure 10 are presented in Table 5. From Table 5, one can conclude that the diffusion coefficient of the imidazolium ring is slightly larger than that of the alkyl chain. This difference is more noticeable for $\text{C}_n(\text{mim})_2(\text{BF}_4)_2$ series than the other DILs. The MSDs of the ring and CT for $\text{C}_n(\text{mim})_2(\text{Br})_2$ do not show any crossing point which indicates that the dynamics of the ring and

the CT atom are identical. However, the MSDs for the $\text{C}_n(\text{mim})_2(\text{PF}_6)_2$, where $n = 6$ and 9, show a crossing point at 6 and 7 ns, respectively. The simulated MSDs of the ring and CT in Figure 10 for $\text{C}_3(\text{mim})_2(\text{PF}_6)_2$ does not show any crossing point. This can be related to the smaller diffusion coefficient of $\text{C}_3(\text{mim})_2(\text{PF}_6)_2$ with respect to the C6 and C9 counterparts. The ring and CT MSDs for $\text{C}_n(\text{mim})_2(\text{BF}_4)_2$ in Figure 10 show well-defined crossing points at times less than 3 ns. The slope of the MSDs of CT is larger than that of the ring for the time periods less than the time of crossing points, but it becomes smaller for time domains larger than the crossing time. For the $\text{C}_n(\text{mim})_2(\text{BF}_4)_2$ DILs the alkyl chain moves faster than the rings in a time scale smaller than 3 ns. However, this time scale for $\text{C}_n(\text{mim})_2(\text{PF}_6)_2$ is as large as 7 ns and for $\text{C}_n(\text{mim})_2(\text{Br})_2$ no crossing point has been observed, so one can conclude that the atoms of the rings move faster than those of the alkyl chain in the time scale of the simulation. The crossing points are sensitive to the proper equilibration and trajectory averaging in the NVE simulations for each ionic liquid. The crossing point for $\text{C}_n(\text{mim})_2(\text{Br})_2$ are difficult to determine with great accuracy since the MSDs of the ring and the alkyl chain are almost parallel to each other. This similarity of the MSDs and diffusion coefficients of the ring and CT indicates that their motion is highly correlated to each other. These results show that the anion has a significant effect on the relative dynamics of the alkyl chain and the imidazolium rings. Our calculated diffusion coefficients in Tables 4 and 5 show that the times of crossing of MSD plots of the ring and alkyl chain in Figure 8 correlate strongly with the diffusion coefficient of the anion. For a fast moving anion, the imidazolium rings move faster than the alkyl chain at the time scales larger than 3–4 ns.

DILs can be used as electrolytes in the electrochemical processes and devices.^{50–54} In most practical electrolyte applications, the relative contributions of the charged species to the transfer of the total charge are also important. For the component 1:2 electrolytes, MX_2 consisting of ions M^{2+} and two X^- , such as the dicationic ionic liquids of interest in this study, transference numbers may be estimated from the diffusion coefficients of the cation and anion

$$t_+ = \frac{D_+}{D_+ + 2D_-}, \quad t_- = \frac{2D_-}{D_+ + 2D_-} \quad (3)$$

The transference numbers were calculated and shown in Table 4. The calculated transference numbers of cation and anion in DILs determined from the MSDs are $0.20 < t_+ < 0.40$ and $0.60 < t_- < 0.80$ respectively, which means that the major contribution to current flow is from anionic transport. Kowsari et al.¹⁰⁵ showed that for the mono cationic ILs $0.49 < t_+ < 0.65$, and it decreases with the alkyl chain length of the cation. The calculated t_+ for DILs in Table 4 are less than 0.5 and decreases with the increasing length of the alkyl chain expect $\text{C}_9(\text{mim})_2\text{Br}_2$. The $t_- > 0.5$ indicates that, unlike the mono cationic ILs, anions have a major role in the transfer of electric current. The larger transference number of the anions can be related to the larger diffusion coefficients of the anion in Table 4, and also that, for a DIL solution, the number of anions is twice that of the cations.

4. CONCLUSION

The molecular dynamic simulation of the $\text{C}_n(\text{mim})_2(\text{X})_2$ dicationic ionic liquids with $\text{X} = \text{BF}_4^-, \text{PF}_6^-, \text{and } \text{Br}^-$ and $n = 3, 6, \text{ and } 9$ were carried out using Canongia-Lopes et al. force

field.⁵⁷ The densities, microscopic structure, vaporization enthalpy, mean square displacement, self-diffusion coefficients, and transference numbers were calculated. The simulated densities using Canongia-Lopes et al. force fields for $C_9(\text{mim})_2(\text{BF}_4)_2$ and $C_9(\text{mim})_2(\text{Br})_2$ agree well with the experimental data. The calculated densities of DILs are greater than that of the mono cationic ILs with the same alkyl chain. The calculated RDFs show that anions tend to spend most of their time around the rings rather than alkyl chain atoms and the anions are very well organized around the cationic rings. Also, we have employed the SDFs to analyze the local structures of $C_9(\text{mim})_2X_2$ ($X = \text{Br}^-$ and PF_6^-) DILs. The visualized SDFs show that anions are clustered around the imidazolium ring where there exists a small low density region around the middle of the alkyl spacer between the two rings. The SDFs around the rings reveals that spatial distribution of anions around the ring is similar with the mono cationic ionic ILs which comprises three high density regions around the imidazolium ring. The observed trends for the diffusion coefficients of cations were $C_3(\text{mim})_2X_2 > C_6(\text{mim})_2X_2 > C_9(\text{mim})_2X_2$ for PF_6^- and Br^- anions and $C_6(\text{mim})_2X_2 > C_9(\text{mim})_2X_2 > C_3(\text{mim})_2X_2$ for BF_4^- . The calculated self-diffusion decreases as the alkyl chain increases except for DILs with anion BF_4^- . Our results show that the order of the diffusion coefficient of anions is as $\text{BF}_4^- > \text{PF}_6^- > \text{Br}^-$. $C_3(\text{mim})_2(\text{BF}_4)_2$ and $C_6(\text{mim})_2(\text{BF}_4)_2$ have the highest ion diffusion coefficients, and they can be used as good charge carriers. The calculated MSDs for the imidazolium rings and the middle carbon of the alkyl chain show that for long time periods the rings move faster than the alkyl chain but in the small time periods the alkyl chain moves faster. The difference between the diffusion rate of the rings and the alkyl chain depends mainly on the nature of the anion and increases with the mobility of the anion. The imidazolium rings act like an anchor for the alkyl chain. The large transfer numbers for anions (0.6–0.8) for DILs show that, unlike the mono cationic ILs, anions have a major role in the transfer of electric current.

■ ASSOCIATED CONTENT

■ Supporting Information

The log–log plots of the MSDs of the ions in the nine ionic liquids are shown in Figures S1–S9. This material is available free of charge via the Internet at <http://pubs.acs.org>.

■ AUTHOR INFORMATION

Corresponding Author

*E-mail: yganegi@umz.ac.ir. Tel.: +98-112-534-2385. Fax: +98-112-534-2350.

Notes

The authors declare no competing financial interest.

■ ACKNOWLEDGMENTS

We acknowledge the University of Mazandaran for financial support of this work. Also we thank Prof. Tom Woo from the University of Ottawa for providing us some computer time.

■ REFERENCES

- (1) Wasserscheid, P.; Keim, W. *Angew. Chem., Int. Ed.* **2000**, *39*, 3772–3789.
- (2) Welton, T. *Chem. Rev.* **1999**, *99*, 2071–2084.
- (3) Cadena, C.; Anthony, J. L.; Shah, J. K.; Morrow, T. I.; Brennecke, J. F.; Maginn, E. J. *J. Am. Chem. Soc.* **2004**, *126*, 5300–5308.
- (4) Anderson, J. L.; Armstrong, D. W. *Anal. Chem.* **2003**, *75*, 4851–4858.
- (5) Anderson, J. L.; Pino, V.; Hagberg, E. C.; Sheares, V. V.; Armstrong, D. W. *Chem. Commun.* **2003**, 2444–2445.
- (6) Fletcher, K. A.; Pandey, S. *Langmuir* **2004**, *20*, 33–36.
- (7) Zhou, Y.; Antonietti, M. *J. Am. Chem. Soc.* **2003**, *125*, 14960–14961.
- (8) Luo, H.; Dai, S.; Bonnesen, P. V.; Buchanan, A. C.; Holbrey, J. D.; Bridges, N. J.; Rogers, R. D. *Anal. Chem.* **2004**, *76*, 3078–3083.
- (9) Wu, J.; Zhang, J.; Zhang, H.; He, J.; Ren, Q.; Guo, M. *Biomacromolecules* **2004**, *5*, 266–268.
- (10) Yang, W.; Fellinger, T. P.; Antonietti, M. *J. Am. Chem. Soc.* **2010**, *133*, 206–209.
- (11) Boxall, D. L.; Osteryoung, R. A. *J. Electrochem. Soc.* **2004**, *151*, 41–45.
- (12) Earle, M. J.; Katdare, S. P.; Seddon, K. R. *Org. Lett.* **2004**, *6*, 707–710.
- (13) Carter, E. B.; Culver, S. L.; Fox, P. A.; Goode, R. D.; Ntai, I.; Tickell, M. D.; Traylor, R. K.; Hoffman, N. W. *Chem. Commun.* **2004**, 630–631.
- (14) Wasserscheid, P.; Hilgers, C.; Keim, W. *J. Mol. Catal. A: Chem.* **2004**, *214*, 83–90.
- (15) Gao, H.; Jiang, T.; Han, B.; Wang, Y.; Du, J.; Liu, Z.; Zhang, Y. *Polymer* **2004**, *45*, 3017–3019.
- (16) Kaar, J. L.; Jesionowski, A. M.; Berberich, J. A.; Moulton, R.; Russell, A. J. *J. Am. Chem. Soc.* **2003**, *125*, 4125–4131.
- (17) Zhao, H.; Malhotra, S. V. *Biotechnol. Lett.* **2002**, *24*, 1257–1260.
- (18) Lee, J. K.; Kim, M. J. *J. Org. Chem.* **2002**, *67*, 6845–6847.
- (19) Wilkes, J. S. *J. Mol. Catal. A: Chem.* **2004**, *214*, 11–17.
- (20) Schopmeyer, H. H.; Felton, G. E.; Ford, C. L. *Ind. Eng. Chem.* **1943**, *35*, 1168–1172.
- (21) Wei, G. T.; Yang, Z.; Lee, C. Y.; Yang, H.-Y.; Wang, C. R. C. *J. Am. Chem. Soc.* **2004**, *126*, 5036–5037.
- (22) Itoh, H.; Naka, K.; Chujo, Y. *J. Am. Chem. Soc.* **2004**, *126*, 3026–3027.
- (23) Liu, W.; Cheng, L.; Zhang, Y.; Wang, H.; Yu, M. *J. Mol. Liq.* **2008**, *140*, 68–72.
- (24) Durrant, J. R.; Haque, S. A. *Nat. Mater.* **2003**, *2*, 362–363.
- (25) Shirota, H.; Fukazawa, H. Atom Substitution Effects in Ionic Liquids: A Microscopic View by Femtosecond Raman-Induced Kerr Effect Spectroscopy. In *Ionic Liquids: Theory, Properties, New Approaches*; Kokorin, A., Ed.; InTech: Rijeka, 2011; p 201.
- (26) Shirota, H.; Castner, E. W., Jr. *J. Phys. Chem. B* **2005**, *109*, 21576–21585.
- (27) Chung, S. H.; Lopato, R.; Greenbaum, S. G.; Shirota, H.; Castner, E. W., Jr.; Wishart, J. F. *J. Phys. Chem. B* **2007**, *111*, 4885–4893.
- (28) Ishida, T.; Nishikawa, K.; Shirota, H. *J. Phys. Chem. B* **2009**, *113*, 9840–9851.
- (29) Shirota, H.; Fukazawa, H.; Fujisawa, T.; Wishart, J. F. *J. Phys. Chem. B* **2010**, *114*, 9400–9412.
- (30) Bradaric, C. J.; Downard, A.; Kennedy, C.; Robertson, A. J.; Zhou, Y. *Green Chem.* **2003**, *5*, 143–152.
- (31) Tsunashima, K.; Sugiyama, M. *Electrochem. Commun.* **2007**, *9*, 2353–2358.
- (32) Tsunashima, K.; Kodama, S.; Sugiyama, M.; Kunugi, Y. *Electrochim. Acta* **2010**, *56*, 762–766.
- (33) Feng, Q.; Huang, K.; Liu, S.; Yu, J.; Liu, F. *Electrochim. Acta* **2011**, *56*, 5137–5141.
- (34) Cho, C. W.; Preiss, U.; Jungnickel, C.; Stolte, S.; Arning, J.; Ranke, J.; Klamt, A.; Krossing, I.; Thöming, J. *J. Phys. Chem. B* **2011**, *115*, 6040–6050.
- (35) Seki, S.; Hayamizu, K.; Tsuzuki, S.; Fujii, K.; Umebayashi, Y.; Mitsugi, T.; Kobayashi, T.; Ohno, Y.; Kobayashi, Y.; Mita, Y.; et al. *Phys. Chem. Chem. Phys.* **2009**, *11*, 3509–3514.
- (36) Anderson, J. L.; Ding, R.; Ellern, A.; Armstrong, D. W. *J. Am. Chem. Soc.* **2005**, *127*, 593–604.
- (37) Liu, Q.; Rantwijk, F.; Sheldon, R. J. *J. Chem. Technol. Biotechnol.* **2006**, *81*, 401–405.

- (38) Jadhav, A. H.; Kim, H.; Hwang, I. T. *Catal. Commun.* **2012**, *21*, 96–103.
- (39) Han, X.; Armstrong, D. W. *Org. Lett.* **2005**, *7*, 4205–4208.
- (40) Xiao, J. C.; Shreeve, J. M. *J. Org. Chem.* **2005**, *70*, 3072–3078.
- (41) Huang, K.; Han, X.; Zhang, X.; Armstrong, D. W. *Anal. Bioanal. Chem.* **2007**, *389*, 2265–2275.
- (42) Anderson, J. L.; Armstrong, D. W. *Anal. Chem.* **2005**, *77*, 6453–6462.
- (43) Liu, T.; Zhang, L. X.; Sun, L. Q.; Luo, A. Q. *Adv. Mater. Res.* **2011**, *382*, 477–480.
- (44) Qi, M.; Armstrong, D. W. *Anal. Bioanal. Chem.* **2007**, *388*, 889–899.
- (45) Chinnappan, A.; Kim, H. *Chem. Eng. J.* **2012**, *187*, 283–288.
- (46) Yu, G. Q.; Yan, S. Q.; Zhou, F.; Liu, X. Q.; Liu, W. M.; Liang, Y. M. *Tribol. Lett.* **2007**, *25*, 197–205.
- (47) Jiménez, A. E.; Bermúdez, M.-D. *Tribol. Lett.* **2009**, *33*, 111–126.
- (48) Jin, C.-M.; Ye, C.; Phillips, B. S.; Zabinski, J. S.; Liu, X.; Liu, W.; Shreeve, J. M. *J. Mater. Chem.* **2006**, *16*, 1529–1535.
- (49) Zhang, Z.; Zhou, H.; Yang, L.; Tachibana, K.; Kamijima, K.; Xu, J. *Electrochim. Acta* **2008**, *53*, 4833–4838.
- (50) Zhang, Z.; Yang, L.; Luo, S.; Tian, M.; Tachibana, K.; Kamijima, K. *J. Power Sources* **2007**, *167*, 217–222.
- (51) Jovanovski, V.; González-Pedro, V.; Giménez, S.; Azaceta, E.; Cabañero, G.; Grande, H.; Tena-Zaera, R.; Mora-Seró, I.; Bisquert, J. *J. Am. Chem. Soc.* **2011**, *133*, 20156–20159.
- (52) Shiota, H.; Ishida, T. *J. Phys. Chem. B* **2011**, *115*, 10860–10870.
- (53) Kim, J. Y.; Kim, T. H.; Kim, D. Y.; Park, N.-G.; Ahn, K.-D. *J. Power Sources* **2008**, *175*, 692–697.
- (54) Ito, K.; Nishina, N.; Ohno, H. *Electrochim. Acta* **2000**, *45*, 1295–1298.
- (55) Pitawala, J.; Matic, A.; Martinelli, A.; Jacobsson, P.; Koch, V.; Croce, F. *J. Phys. Chem. B* **2009**, *113*, 10607–10610.
- (56) Zeng, Z.; Phillips, B. S.; Xiao, J. C.; Shreeve, J. M. *Chem. Mater.* **2008**, *20*, 2719–2726.
- (57) Shiota, H.; Mandai, T.; Fukazawa, H.; Kato, T. *J. Chem. Eng. Data* **2011**, *56*, 2453–2459.
- (58) Sun, H.; Zhang, D. J.; Liu, C. B.; Zhang, C. Q. *J. Mol. Struct. (THEOCHEM)* **2009**, *900*, 37–43.
- (59) Nooruddin, N. S.; Wahlbeck, P. G.; Carper, W. R. *Tribol. Lett.* **2009**, *36*, 147–156.
- (60) Dommert, F.; Wendler, K.; Berger, R.; Delle Site, L.; Holm, C. *ChemPhysChem* **2012**, *13*, 1625–1637.
- (61) Canongia-Lopes, J. N.; Deschamps, J.; Pádua, A. H. *J. Phys. Chem. B* **2004**, *108*, 2038–2047.
- (62) Liu, X.; Zhang, S.; Zhou, G.; Wu, G.; Yuan, X.; Yao, X. *J. Phys. Chem. B* **2006**, *110*, 12062–12071.
- (63) Bodo, E.; Caminiti, R. *J. Phys. Chem. A* **2010**, *114*, 12506–12512.
- (64) Bhargava, B. L.; Klein, M. L. *J. Chem. Theory Comput.* **2010**, *6*, 873–879.
- (65) Bhargava, B. L.; Klein, M. L. *J. Phys. Chem. B* **2011**, *115*, 10439–10446.
- (66) Bodo, E.; Chiricotto, M.; Caminiti, R. *J. Phys. Chem. B* **2011**, *115*, 14341–1437.
- (67) Frisch, M. J.; et al. *Gaussian 03*, revision C.02; Gaussian, Inc.: Wallingford, CT, 2004.
- (68) Smith, W.; Forester, T. R.; Todorov, I. T. *DL POLY*, v2.20; Daresbury Laboratories, 2009.
- (69) Nose, S. *J. Chem. Phys.* **1984**, *81*, 511–519.
- (70) Hoover, W. G. *Phys. Rev. A* **1985**, *31*, 1695–1697.
- (71) Allen, M. P.; Tildesley, D. J. *Computer Simulations of Liquids*; Oxford University Press: Oxford, U.K., 1987.
- (72) Liu, Z.; Wu, X.; Wang, W. *Phys. Chem. Chem. Phys.* **2006**, *8*, 1096–1104.
- (73) Tariq, M.; Forte, P. A. S.; Costa Gomes, M. F.; Canongia-Lopes, J. N.; Rebelo, L. P. N. *J. Chem. Thermodyn.* **2009**, *41*, 790–798.
- (74) Seddon, K.; Stark, A. *Alternative Media for Chemical Reactions and Processing*. ACS Symposium Series 819; American Chemical Society: Washington, DC, 2002.
- (75) Kelkar, M. S.; Maginn, E. J. *J. Phys. Chem. B* **2007**, *111*, 9424–9427.
- (76) Leal, J. P.; Esperanca, J.; da Piedade, M. E. M.; Canongia-Lopes, J. N.; Rebelo, L. P. N.; Seddon, K. R. *J. Phys. Chem. A* **2007**, *111*, 6176–6182.
- (77) Strasser, D.; Goulay, F.; Kelkar, M. S.; Maginn, E. J.; Leone, S. R. *J. Phys. Chem. A* **2007**, *111*, 3191–3195.
- (78) Lovelock, K. R. J.; Deyko, A.; Corfield, J.-A.; Gooden, P. N.; Licence, P.; Jones, R. G. *ChemPhysChem* **2009**, *10*, 337–340.
- (79) Vitorino, J.; Leal, J. P.; Licence, P.; Lovelock, K. R. J.; Gooden, P. N.; Minas da Piedade, M. E.; Shimizu, K.; Rebelo, L. P. N.; Canongia Lopes, J. N. *ChemPhysChem* **2010**, *11*, 3673–3677.
- (80) Morrow, T. I.; Maginn, E. J.; Field, F. J. *J. Phys. Chem. B* **2002**, *106*, 12807–12813.
- (81) Deyko, A.; Lovelock, K. R. J.; Corfield, J. A.; Taylor, A. W.; Gooden, P. N.; Villar-Garcia, I. J.; Licence, P.; Jones, R. G.; Krasovskiy, V. G.; Chernikova, E. A.; et al. *Phys. Chem. Chem. Phys.* **2009**, *11*, 8544–8555.
- (82) Bhargava, B. L.; Klein, M. L. *J. Phys. Chem. A* **2009**, *113*, 1898–1904.
- (83) Urahata, S. M.; Ribeiro, M. C. C. *J. Chem. Phys.* **2004**, *120*, 1855–1863.
- (84) Bhargava, B. L.; Klein, M. L. *J. Phys. Chem. B* **2009**, *113*, 9499–9505.
- (85) Resende Prado, C. E.; Gomide Freitas, L. C. *J. Mol. Struct.* **2007**, *847*, 93–100.
- (86) Bankmann, D.; Giernoth, R. *Progr. Magn. Res. Spectrosc.* **2007**, *51*, 63–90.
- (87) Huang, J.; Chen, P.; Sun, L.; Wang, S. P. *Inorg. Chim. Acta* **2001**, *320*, 7–11.
- (88) Zhao, W.; Leroy, F.; Heggen, B.; Zahn, S.; Kirchner, B.; Balasubramanian, S.; Müller-Plathe, F. *J. Am. Chem. Soc.* **2009**, *131*, 15825–15833.
- (89) Noack, K.; Leipertz, A.; Kiefer, J. *J. Mol. Struct.* **2012**, *1018*, 45–53.
- (90) Dong, K.; Zhang, S. *Chem.—Eur. J.* **2012**, *18*, 2748–2761.
- (91) Kanzaki, R.; Takushi, M.; Shuhei, F.; Kenta, F.; Munetaka, T.; Yasufumi, S.; Toshiyuki, T.; Toshio, Y.; Yasuhiro, U.; Shin-ichi, I. *J. Mol. Liq.* **2009**, *147*, 77–82.
- (92) Youngs, T. G. A. *J. Comput. Chem.* **2010**, *31*, 639–648.
- (93) Raabe, G.; Köhler, J. *J. Chem. Phys.* **2008**, *128*, 154509.
- (94) Del Pópolo, M. G.; Voth, G. A. *J. Phys. Chem. B* **2004**, *108*, 1744–1752.
- (95) Umebayashi, Y.; Hamano, H.; Tsuzuki, S.; Canongia Lopes, J. N.; Pádua, A. A. H.; Kameda, Y.; Kohara, S.; Yamaguchi, T.; Fujii, K.; Ishiguro, S. *J. Phys. Chem. B* **2010**, *114*, 11715–11724.
- (96) Bhargava, B. L.; Balasubramanian, S. *J. Phys. Chem. B* **2007**, *111*, 4477–4487.
- (97) Liu, Z.; Huang, S.; Wang, W. *J. Phys. Chem. B* **2004**, *108*, 12978–12989.
- (98) Hardacre, C.; McMath, S. E. J.; Nieuwenhuyzen, M.; Bowron, D. T.; Soper, A. K. *J. Phys.: Condens. Matter* **2003**, *15*, S159.
- (99) Frenkel, D.; Smit, B. *Understanding Molecular Simulation*; Academic Press: New York, 1996.
- (100) Tsuzuki, S.; Shinoda, W.; Saito, H.; Mikami, M.; Tokuda, H.; Watanabe, M. *J. Phys. Chem. B* **2009**, *113*, 10641–10649.
- (101) Machida, H.; Sato, Y.; Smith, R. L. *Fluid Phase Equilib.* **2008**, *264*, 147–155.
- (102) Tsuzuki, S.; Matsumoto, H.; Shinoda, W.; Mikami, M. *Phys. Chem. Chem. Phys.* **2011**, *13*, 5987–5993.
- (103) Borodin, O. *J. Phys. Chem. B* **2009**, *113*, 11463–11478.
- (104) Borodin, O.; Smith, G. D. *J. Phys. Chem. B* **2006**, *110*, 11481–11490.
- (105) Kowsari, M. H.; Alavi, S.; Ashrafzaadeh, M.; Najafi, B. *J. Chem. Phys.* **2008**, *129*, 224508–224521.